ACOUSTIC CHARACTERISTICS OF FATIGUED ALUMINUM ALLOY USING ULTRASONIC SHEAR WAVES

H. Yamagishi [1], and M. Fukuhara [2]

[1]Central Research Institute, Toyama Industrial Technology Center, Takaoka, 933-0981, Japan

[2] Institute for Materials Research, Tohoku University, Sendai, 980-8577, Japan

ABSTRACT

Cyclic-tension fatigue of aluminum alloy, Al-4Cu-1Mg, was determined by an analysis of diffracted SH and SV waves, passing through the surface and reflecting the bottom of the specimen, respectively. The internal friction of SV waves begins to increase from fatigue damage ratio(=N/N$_f$) of 0.5. This suggests increase of movable dislocation. From the analysis of SH waves, the logarithmic damping ratio and the propagation time decreases with increasing of the degree of fatigue. Assumed from SH wave flux model, the residual stress field applied by cyclic-tension makes the damping ratio and the propagation time decrease. The experimental result correlates well with this theory. These results show that ultrasonic method is useful probe for evaluation of fatigue in aluminum alloy.

KEYWORDS; *fatigue, aluminum alloy, cyclic tension, nondestructive inspection, acoustic characteristic*

1. INTRODUCTION

When engineering metals are subjected to fluctuating loads in service, they are liable to fracture by fatigue, the most common of all causes of engineering failure [1-3]. Thus there have been extensive efforts to relate observed data using X-ray diffraction [4-6], positron annihilation [7,8], laser diffusion [9], ultrasonic transmission [10-12], acoustic emission [13,14], hardness [15] methods to evaluate the actual fatigue level in materials. However, conventional methods are not necessarily satisfactory to predict the damage of fatigued materials for field application.

To develop a nondestructive inspection technique for fatigue, we have investigated acoustic characteristics of an aluminum alloy, using horizontally polarized shear wave and vertically polarized shear wave (here after referred to as SH and SV wave, respectively) [16].

The shear waves are known as sensitive to even atomic or molecule level material change [17]. SH wave has polarized plane which is parallel to the interface when it propagates with the angle of incident, that is, the transmission wave is easy to propagate under the target surface. And as further advantage, it does not transform its wave mode from shear wave to longitudinal wave, just remains shear wave mode [18].

In this study, we selected the aluminum alloy as fatigued material, because it is the most commonly used light-metal that fatigue evaluation has not fully developed.

2. EXPERIMENTAL

2.1. MATERIAL

The material used in this study was Al-4Cu-1Mg alloy (JIS-A2024, temper T3) supplied by Corus Aluminum Walzprodukte GmbH. The chemical composition and mechanical prosperities of material are shown in Table 1 and Table 2, respectively. The specimen configuration, which originally designed for fatigue tests, is shown in Fig. 1. The specimen is a flat-rolled bar with a narrow part for break.

Material	Si	Fe	Cu	Mn	Mg	Cr	Zn	Ti	Ti+Zr	Others each	Others total	Al
JIS A2024	0.057	0.127	4.334	0.585	1.457	0.004	0.038	0.029	0.031	0.008	0.028	Bal.

Table 1. Chemical composition of material [mass %]

Temper	0.2%Proof stress [MPa]	Tensile strength [MPa]	Elongation [%]
T3	316	459	17.2

Table 2. Mechanical prosperities of material

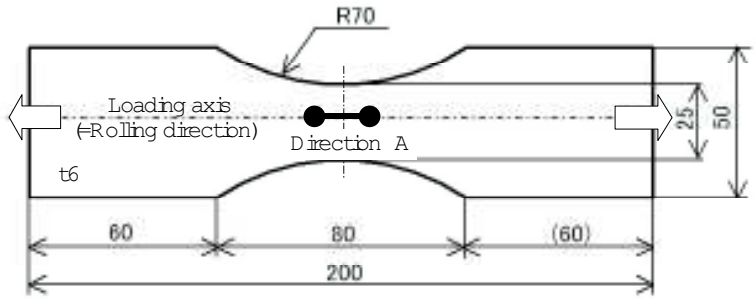

Fig. 1. Configuration of the tension test specimen (dimension in mm).

2.2. EXPERIMENTAL METHODS

Specimen was subjected to a cycle stress amplitude of 233 MPa under load control with 30 Hz frequency in monaxial tensile mode at room temperature, to apply fatigue damage. The fatigue tests were interrupted at various cycles to obtain fatigued specimens having different damages. After specified number of cycles, $N/N_f = 0 \square 0.995$ (N: number of cycles, N_f: number of cycles to failure=3.72×10^5), the waveform deviation between the contact line, Direction A, in the center sections of specimen (Fig. 1) was measured by the use of a bridge with an ultrasonic transmitter/receiver set (Fig. 2). Ultrasonic wave pattern analysis was made by diagnosis and analyzing apparatus (Toshiba Tungaloy).

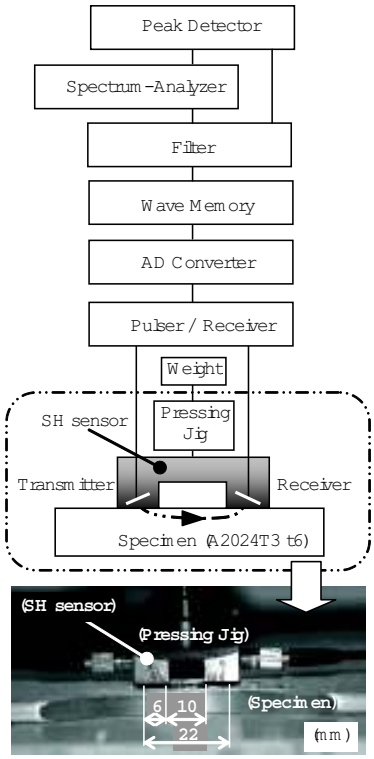

Fig. 2. Schematic diagram for measurement.

The apparatus and a block diagram for the measurement are presented schematically in Fig. 2. Facing narrow-band width SH wave transducers, with probe area of 6 mm×6 mm, were used as the transmitter and the receiver. The two facing transducers in the bridge were arranged by a ditch of 10 mm width. The incident and receiving angles of the SH waves were fixed at 21° which gives maximum receiving amplitude derived from following formula:

$$\frac{Sin\theta_1}{V_1} = \frac{Sin\theta_2}{V_2} \tag{1}$$

where $Sin\theta_1$ and $Sin\theta_2$ are incident and refracting angles for boundary normal, respectively. V_1 and V_2 are shear wave velocities of contacting material of piezoelectric element and pure aluminum, respectively. θ_2 is designed for surfacewave, *i.e.*, critical angle 90°. In order to prevent propagation loss due to high frequency and signal broading due to low frequency, a frequency of 5 MHz was selected as center frequency of transducer. The transducer was contacted at one edge of specimen under a pressure of 3.1 MPa, by water-free naphthenic hydrocarbon oil (Tungsonic Oil H [19]).

Fig. 3 shows a representative SH waveform pattern. We measured the position of the 1st wavelet as propagation time T1. The logarithmic damping ratio, ln(P1/P2), was calculated from amplitude.

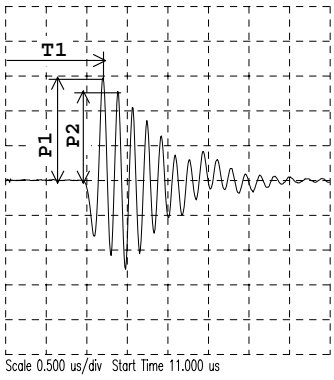

Fig. 3. Example of a receiving waveform using SH sensor.

The internal friction at the center of the specimen was measured by SV wave with frequency of 5 MHz at room temperature. The logarithmic damping δ was determined by the form:

$$\delta = \ln\left(\frac{A_1}{A_2}\right) \tag{2}$$

where A_1 and A_2 are 1st and 2nd amplitudes of the receiving waves, respectively.
The internal friction Q_s^{-1} is defined by the following formula:

$$Q_s^{-1} = \frac{V_s \ln\left(\frac{A_1}{A_2}\right)}{2\pi lf} \tag{3}$$

where Vs is the sound velocity of SV wave. l is the thickness of the specimen and f is the center frequency.

3. RESULTS AND DISCUSSION

The relationship of propagation time, logarithmic damping ratio and internal friction for fatigue damage ratio N/N_f is shown in Fig. 4. Finally, the propagation time decreases with fluctuating on the way. Likewise, the logarithmic damping ratio decreases as the fatigue increases and its trend is clearer than the propagation time. On the other hand, the internal friction does not change significantly until 0.5 of N/N_f. However, exceeding about 0.5 of N/N_f, the internal friction increases rapidly to the break. Furthermore, we can recognize the characteristic correlation between the propagation time and the logarithmic damping ratio in this range.

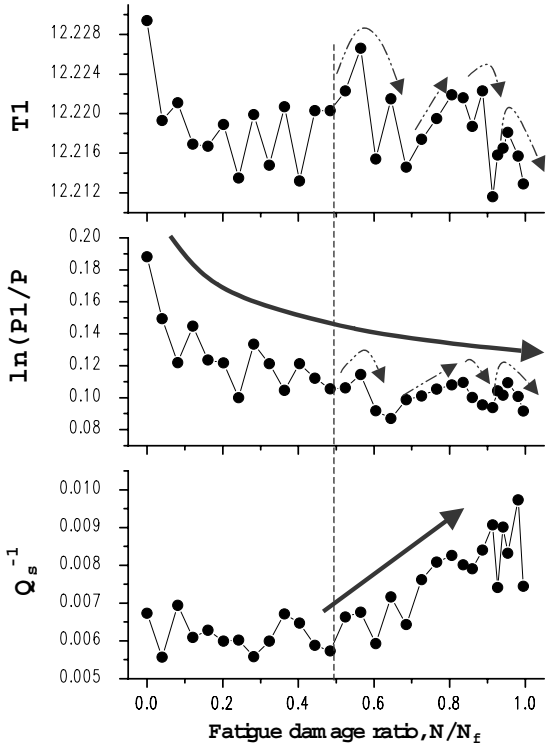

Fig. 4 Relationship for fatigue damage ratio of propagation time, logarithmic damping ratio and internal friction.

Here we consider a relation between fatigued degree and internal friction in terms of energy consumption by dislocation motion. Koehler [20], Granato and Lücke [21] produced KGL model expressing dislocation motion by assuming elastic string model under the condition of viscoelasticity. According to KGL model, the internal friction is leaded by the following equations [22]:

$$A\frac{\partial^2 u}{\partial t^2}+B\frac{\partial u}{\partial t}-C\frac{\partial^2 u}{\partial x^2}=\square \quad (4)$$

where *u, A, B, C* and *b* are displacement, effective mass per unit length, viscous resistance, line tension and Burgers vector, respectively. The solution of normal vibration is expressed in the following form:

$$u=\frac{4b\square}{\square A}\sin(\frac{\square}{L}x)\frac{\exp[i(\square-\square)]}{\sqrt{(\square-\square)^2+(\square)^2}},\quad (\square=\left(\frac{\square}{L}\right)\sqrt{\frac{C}{A}},\tan\square=\frac{\square}{(\square-\square)},d=\frac{B}{A}) \quad (5)$$

where *L* is transposition length. On the assumption that all transposition lengths are the same, the distortion ε_d caused by dislocation displacement is calculated by the following form:

$$\varepsilon_d=\frac{\Lambda b}{L}\int_0^L u dx \quad (6)$$

where Λ is dislocation density. Substituting Eq. (4) into Eq. (5), the internal friction is leaded by following form:

$$Q^{-1}\approx\frac{\square\Lambda L^2}{\square}\left[\frac{w_0^2 wd}{\left(w_0^2-w^2\right)^2+\left(wd\right)^2}\right],\quad \square=\frac{8\square}{\square C}) \quad (7)$$

whereμ is shear modulus. As from N/N_f=0.5 of Fig. 4 according to the internal friction form of Eq. (7), the rapid increasing point in internal friction suggests the drastic change of material in terms of fatigue. Thus it seems that measurement of internal friction become a probe for evaluation of fatigue.

Second, we consider a relation between fatigued degree, logarithmic damping ratio and propagation time in terms of acoustoelasticity. If a two-dimensional x-y plate to which a stress is applied in the x and y directions of a cartesian coordinate system (x, y, z) (Fig. 5), where a residual stress exists in the plate, the acoustic energy flow P of the SH waves propagating in the x-y plane at an arbitrary angle α from the specimen surface can be expressed in the following form [23];

$$P=\sqrt{P_x^2+P_y^2}=\sqrt{\left(\frac{1}{2}u\square\right)^2+\left(\frac{1}{2}u\square\right)^2} \quad (8)$$

$$\alpha=\tan^{-1}\frac{P_y}{P_x}=\tan^{-1}\frac{\square}{\square} \quad (9)$$

$$\frac{\partial u}{\partial}$$

$$u = A\exp[i\xi(x\sin\theta - ct + \beta z)] \quad (11)$$

where P_x and P_y are energy flux of direction x and direction y, respectively. u is the displacement of SH wave to direction z. τ_{xz} and τ_{yz} are shearing stress of direction z at x plane and y plane, respectively. μ, A, ξ *and* β are shear modulus, displacement amplitude, number of waves, element of wave number to direction z, respectively. As can be seen from decrease in damping of Fig. 4 and the energy flux angle of Eq. (9) and considering the simulation result that the energy flow of SH wave bends to more interior as the deeper it propagates [24], it is clear that the incident waves shift to the specimen surface with increasing residual stress as the degree of fatigue, *i.e.*, the crystal lattice distortion by tensile stress. Fig.6 shows relationship between fatigue damage ratio and its residual stress measured by X-ray diffraction (XRD) under the same load condition of SH and SV test. From this result, as expected, it is obvious that the residual stress build up as tensile side with increasing of the degree of fatigue. So it is summarized that the logarithmic damping ratio, ln(P1/P2), decreases with the increase of cyclic-tension fatigue, *i.e.,* the increase of residual stress in tensile side. Considering this conclusion and the characteristic synchronous between propagation time and logarithmic damping ratio, it is also obvious that the propagation time is influenced strongly by the residual stress. *i.e.,* the transmission path of SH wave is leaded by residual stress (Fig. 7).

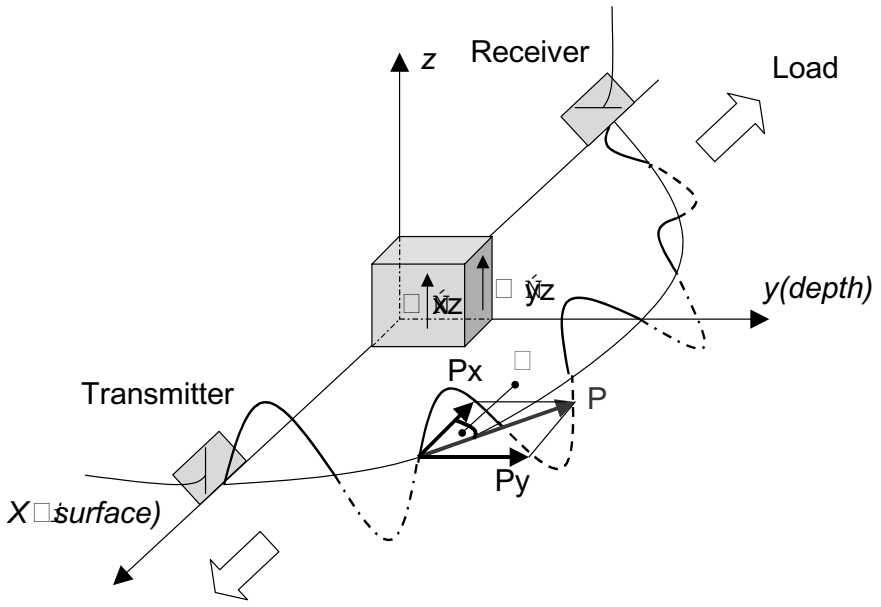

Fig.5 Energy flux of SH wave.

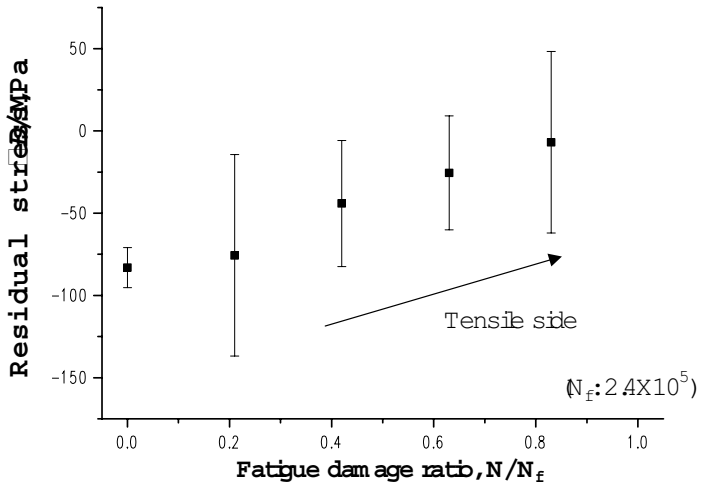

Fig. 6. Relationship between fatigue damage ratio and residual stress.

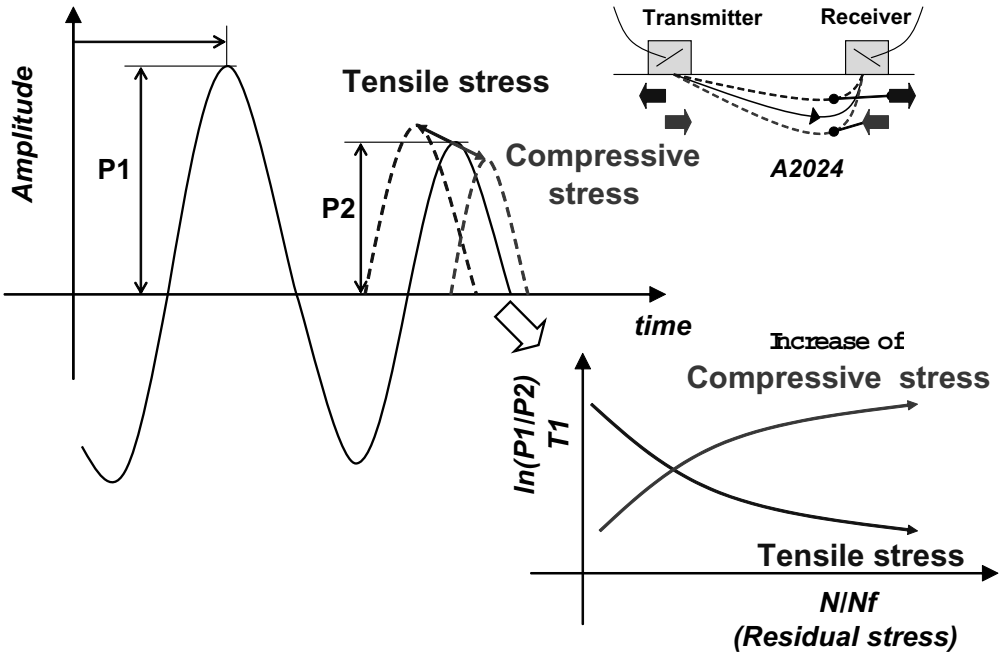

Fig.7. Relationship for the residual stress of logarithmic damping and propagation time.

4. CONCLUSION

In this study, we analyzed the wave patterns of SH and SV waves propagating through cyclic-tension fatigued alloy, Al-4Cu-1Mg, in view of viscoelasticity and acoustoelasticity. The internal friction increases as the number of cycles increases over N/N_f=0.5. This suggests increasing in movable dislocations, *i.e.*, the drastic change of material in terms of fatigue. Furthermore the logarithmic damping ratio and the propagation time decrease with increasing fatigue. Assumed from SH wave flux model, the crystal lattice distortion by the tensile stress makes the energy flow of SH wave bend to specimen surface. *i.e.*, the residual stress field applied by cyclic tension makes the damping ratio and the propagation time decrease. Detecting the acoustic characteristics along the direction to the loading axis, the ultrasonic SH wave method is suitable probe for fatigue evaluation in aluminum alloy.

REFERENCES

[1] S. Fujiki: *How to look at the fractured surface due to fatigue*, (Nikkankougyou, Tokyo, 2002) pp. 2-4

[2] S. Fujiki: Maintenance, **135** (1991) 25-29

[3] K. Mori et al.: *Fractography*,(Maruzen, Tokyo, 2000) pp. 136-137

[4] T. Ungar, G. Ribarik, J. Gubicza and P. Hanak: Trans. ASME. J. Eng. Mater. Technol., **124** (2002) 2-6

[5] P. J. Withers: Mater. Sci. Technol., **17** (2001) 759-765

[6] A. Olchini, H. Stamm and F. D. S. Marques: Surf. Eng., **14** (1998) 386-390

[7] F. Hori: Applied Surf. Sci., **242** (2005) 304-312

[8] Y. Kawaguchi and S. Yasuharu: J. Nucl. Sci. Technol., **39** (2002) 1033-1040

[9] A. Kato and F. Okutani: Collected papers of the Japanese society of the mechanical engineers for materials and mechanics division, (2002) pp. 193-194

[10] E. R. Reinhart, S. Kaminski and M. Monaco: Pap. Summ. ASNT. Conf. Qual. Test. Show, (2005) pp. 339-346

[11] J. Frouin, S. Sathish, T. E. Matikas and J. K. Na: J. Mater. Res., **14** (1999) 1295-1298

[12] H. Ogi, T. Hamaguchi and M. Hirao: Metall. Mater. Trans., **31A** (2000) 1121-1128

[13] Z. Shi, J. Jarzynski, S. Bair, S. Hurlebaus and L. J. Jacobs: Proc. Inst. Mech. Eng. Part C, **214** (2000) pp. 1141-1149

[14] J. P. Bonnafe, G. Maeder and Bathiasc: Proc. 3rd Int. Conf. on Shot Peening, (1987) pp. 485-497

[15] H. Hattori, M. Kitagawa and K. Sugai: Current Advances in Materials and Processes, **1** (1988) 901

[16] H. Yamagishi and M. Fukuhara: Mater. Trans., **48**(2007)550-555
[17] M. Fukuhara and A. Sanpei: Phys.Rev., **B49** (1994) 99-105
[18] H. Fukuoka, H. Toda and M. Hirao: *Basis and application of acoustoelasticity*, (Ohmsha, Tokyo, 1993) pp.18-19
[19] M. Fukuhara and T. Tsubouchi, Chem. Phys. Lett., **371** (2003) 184
[20] J. S. Koehler: *Imperfections in Nearly Perfect Crystals*, (John Wiley and Sons inc., New York, 1952) pp.197
[21] A. Granato and K. Lücke: J.Appl.Phy, **27** (1956) 583-593
[22] O. Izumi et al.: *Atomic theory for strength of materials*, (The Japan Institute of Metals, Tokyo, 1985) pp.77-78
[23] M. Fukuhara, Y. Kuwano, K. Saito and I. Furumura: Collected abstracts of the 1996 Autumn meeting of the Japanese society for non-destructive inspection, (1996) pp.175-178
[24] H. Toda, J. Jpn. Soc. Nondestructive Inspection, **40** (1991) 415-420

Corresponding author:
Email; yamagisi@itc.pref.toyama.jp
Tel.; +81-766-21-2121 / Fax.; +81-766-21-2402